



**HAL**  
open science

## Chalcogen OCF 3 Isosteres Modulate Drug Properties without Introducing Inherent Liabilities

Clément Ghiazza, Thierry Billard, Callum Dickson, Anis Tlili, Christian Gampe

► **To cite this version:**

Clément Ghiazza, Thierry Billard, Callum Dickson, Anis Tlili, Christian Gampe. Chalcogen OCF 3 Isosteres Modulate Drug Properties without Introducing Inherent Liabilities. *ChemMedChem*, 2019, 14 (17), pp.1586-1589. 10.1002/cmdc.201900452 . hal-03035756

**HAL Id: hal-03035756**

**<https://hal.science/hal-03035756>**

Submitted on 21 Dec 2020

**HAL** is a multi-disciplinary open access archive for the deposit and dissemination of scientific research documents, whether they are published or not. The documents may come from teaching and research institutions in France or abroad, or from public or private research centers.

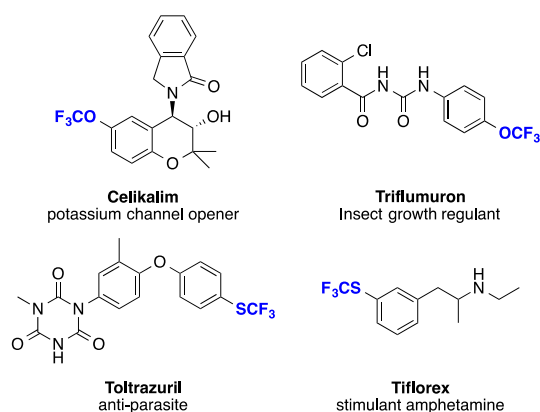
L'archive ouverte pluridisciplinaire **HAL**, est destinée au dépôt et à la diffusion de documents scientifiques de niveau recherche, publiés ou non, émanant des établissements d'enseignement et de recherche français ou étrangers, des laboratoires publics ou privés.

# Chalcogen OCF<sub>3</sub>-isosteres Modulate Drug Properties without Introducing Inherent Liabilities

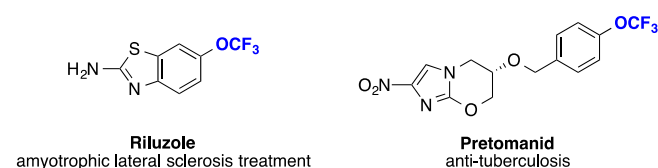
Clément Ghiazza,<sup>[a]</sup> Thierry Billard,<sup>[a, b]</sup> Callum Dickson<sup>[c]</sup>, Anis Tlili<sup>\*[a]</sup> and Christian M. Gampe<sup>\*[c]</sup>

**Abstract:** The synthesis of SCF<sub>3</sub> as well as SeCF<sub>3</sub> isosteres of two OCF<sub>3</sub>-containing drugs was achieved through visible light and copper-catalyzed processes. Herein, we show that chalcogen replacement modulates physico-chemical and ADME properties without introducing intrinsic liabilities. The S- and SeCF<sub>3</sub> groups are more lipophilic than their O-parent; however, microsomal stability is unchanged, indicating that these molecular changes may be beneficial for in vivo half-life. Enabled by modern synthetic methods, we present the chalcogen-CF<sub>3</sub> groups as potential key players for future fluorinated pharmaceuticals.

Organofluorine chemistry gained widespread interest since its discovery in the last century. The advantage relies on the gained properties including the increased stability against oxidative metabolism as well as the lipophilicity.<sup>[1]</sup> Moreover, fluorine is routinely used as a bioisoster of hydrogens or hydroxyl groups in drug design.<sup>[2]</sup> In parallel, attention has been turned recently to the incorporation of trifluoromethyl chalcogen groups into organic molecules in order to tune the physicochemical properties. Historically, indirect approaches have been used and several active compounds are already finding a plethora of applications. In the forefront, trifluoromethoxylated compounds are employed in all areas of life science.<sup>[3]</sup> To date, several compounds are in the market. In contrast, compounds with SCF<sub>3</sub> group are scarcely studied,<sup>[4]</sup> and, to the best of our knowledge, there is no biologically active compound on the market containing SeCF<sub>3</sub> (Scheme 1).<sup>[5]</sup> During the past years, we have been involved in the design as well as the use of new reagents for trifluoromethyl chalcogenation. Our focus has been lately on the scarcely studied SeCF<sub>3</sub> motif, and we recently reported photocatalytic and copper-catalyzed strategies to access the aryl-SeCF<sub>3</sub> motif by using our reagent, namely trifluoromethylselenosulfonate.<sup>[6]</sup> Herein, we report the application of these processes in the synthesis of the chalcogen homologs of Riluzole and Pretomanid, two bioactive molecules bearing OCF<sub>3</sub> moieties, as well as their physicochemical and in vitro ADME properties, and their off-target profiles. Riluzole is already commercialized for amyotrophic lateral sclerosis treatment,<sup>[7]</sup> and a New Drug Application has recently been accepted by the FDA for the treatment of tuberculosis with Pretomanid (PA-824) (Scheme 2).<sup>[8]</sup>



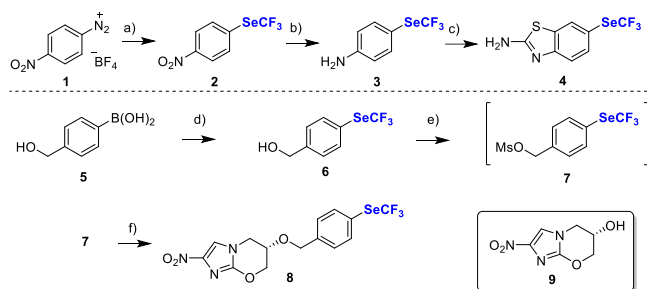
**Scheme 1.** Examples of trifluoromethoxylated and trifluoromethylthiolated, commercial bioactive compounds



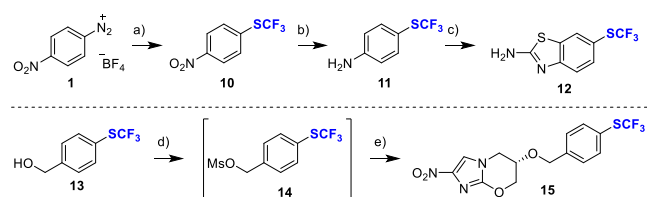
**Scheme 2.** Pharmacologically active compounds chosen as test cases for the effects of the replacement of OCF<sub>3</sub> with SCF<sub>3</sub> and SeCF<sub>3</sub>

The selenylated analog of Riluzole was first prepared (Scheme 3, top). In a visible-light metal-free procedure, using Eosin Y as organic photocatalyst, aryl diazonium salt **1** was combined with the trifluoromethylselenolating agent TsSeCF<sub>3</sub> under white LED irradiation. This procedure allows the formation of the desired product **2** in 75 % yield.<sup>[6b]</sup> Afterwards, the reduction of the nitro moiety was performed with iron powder in aqueous HCl media leading to the corresponding aniline **3** with 81 % yield within 1 hour.<sup>[9]</sup> Finally, Se-Riluzole analog **4** was obtained after a cyclization with bromine and potassium thiocyanate in acetic acid with an overall yield of 40 %.<sup>[10]</sup>

The Se-Pretomanid derivative was prepared in a three steps sequence (Scheme 3, bottom). First, commercially available boronic acid **5** was converted to the trifluoromethylselenylated arene **6** under copper catalysis with a moderate yield.<sup>[6a]</sup> Next, the benzyl alcohol was mesylated. Afterwards, removal of both NEt<sub>3</sub> as well as the excess of MsCl was undertaken. Finally, Se-Pretomanid **8** was obtained by mixing **7** with commercially available and enantiopure alcohol **9** in the presence of sodium hydride furnishing the desired compounds in overall yield of 30 %.



**Scheme 3.** Se-Riluzole and Se-Pretomanid syntheses. a) TsSeCF<sub>3</sub> (3 equiv.), eosin Y (5 mol%), DMSO, rt, 16 h, white LED, 75 %. b) Fe (3.5 equiv.), HCl 37 % (10 equiv.) 90 °C, 1 h, 81 %. c) KSCN (4 equiv.), Br<sub>2</sub> (1 equiv.), AcOH, rt, 16 h, 66 %. d) TsSeCF<sub>3</sub> (1 equiv.), Cu(OAc)<sub>2</sub> (10 mol%), bpy (10 mol%), Cs<sub>2</sub>CO<sub>3</sub> (1 equiv.), THF, rt, 16 h, 45 %. e) NEt<sub>3</sub> (4 equiv.), MsCl (2 equiv.), CH<sub>2</sub>Cl<sub>2</sub>, 0 °C, 30 min. f) **9** (1 equiv.), NaH (2 equiv.), DMF, rt, 16 h, 66%.

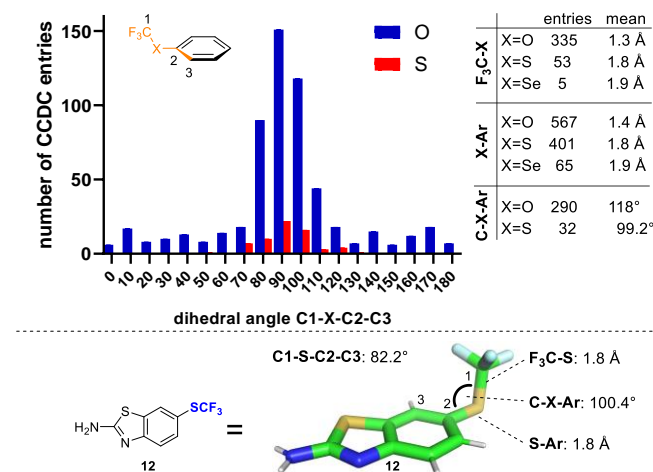


**Scheme 4.** S-Riluzole and S-Pretomanid syntheses. a) TsSCF<sub>3</sub> (3 equiv.), [Ru(phen)<sub>3</sub>Cl<sub>2</sub>] (5 mol%), DMSO, rt, 16 h, white LED, 50 %. b) Fe (3.5 equiv.), HCl 37 % (10 equiv.) 90 °C, 1 h, 73 %. c) KSCN (4 equiv.), Br<sub>2</sub> (1 equiv.), AcOH, rt, 16 h, 54 %. d) NEt<sub>3</sub> (4 equiv.), MsCl (2 equiv.), CH<sub>2</sub>Cl<sub>2</sub>, 0 °C, 30 min. f) **9** (1 equiv.), NaH (2 equiv.), DMF, rt, 16 h, 66%.

Sulfur analogs were synthesized using similar procedures. Trifluoromethylthiolated arene **10** was prepared from the corresponding diazonium salt **1** with a Ru-based photocatalyst with a moderate yield of 50 % (Scheme 4, top).<sup>[11]</sup> Nitro reduction was then performed with good efficiency, and aniline **11** was obtained in 73 % yield. The desired compound **12** was isolated after the third step with an overall yield of 20 %. The synthesis of Se-Pretomanid started with commercially available trifluoromethylthiolated arene **13** (Scheme 4, bottom). A sequential mesylation/substitution with **9** allowed us to prepare the desired product **15** in 66 % yield.

Isosteric replacement of functional groups is a powerful strategy in medicinal chemistry to modulate physicochemical and ADME properties while retaining on-target potency.<sup>[12]</sup> Since molecular structure determines properties, bioisosteres need to strike a balance: Structural and electronic differences between the isostere and the parent functional group must be small enough to enable recognition by the biological target but large enough to significantly change other properties. Thus, we set out to assess the influence of chalcogen replacement in aryl-OCF<sub>3</sub>-containing compounds on structure and electronic properties. First, we performed a search for bond lengths and angle distributions in x-ray crystal structures of Ar-X-CF<sub>3</sub> containing compounds in the Cambridge Crystallographic Data Centre database using the Mogul Software (Scheme 5, top). We found that both sigma-bonds, the F<sub>3</sub>C-X and X-Ar bonds, significantly increase in length going from X=O (ca. 1.4 Å) to X=S (ca. 1.8 Å). The corresponding bonds in the selenium-containing structures are only marginally longer (ca. 1.9 Å). The mean bond angle at the chalcogen decreases from 118° in F<sub>3</sub>C-O-Ar to 99.2° in F<sub>3</sub>C-S-Ar compounds (no entries for the Se-homolog were found). When the dihedral angle of F<sub>3</sub>C-X-C was assessed, we saw a clear preference of the CF<sub>3</sub>-group to adopt a conformation perpendicular to the aromatic plane for both OCF<sub>3</sub> and SCF<sub>3</sub> groups; although significantly less CCDC entries exist for the sulfur derivatives than for the OCF<sub>3</sub>-compounds. Only two values for the dihedral angle in ArSeCF<sub>3</sub> structures are listed in the CCDC database, both close to 90°. We obtained an

x-ray crystal structure of compound **12** and found the geometry around the SCF<sub>3</sub> group to be comparable to the mean values obtained from the CCDC (Scheme 5, bottom). Next, we assessed the influence of chalcogen replacement on electronics via quantum mechanical calculations. We did not find significant differences in the dipole moments, electron densities, or the HOMO-LUMO gaps for the Pretomanid and Riluzole chalcogen matched pairs (see SI for details). Taken together with the structural information, we concluded that chalcogen replacement does not overly perturb conformation and electronics of the molecules, suggesting that desired biological activity may be conserved. However, if structural differences manifest in property differences we would expect the sulfur and selenium derivatives to be more similar to one another than to the Ar-OCF<sub>3</sub>-compounds.



**Scheme 5.** While structural and conformational trends are generally conserved between chalcogen homologs, differences between OCF<sub>3</sub>- and SCF<sub>3</sub>-compounds are larger than between SCF<sub>3</sub>- and SeCF<sub>3</sub>-compounds. Cambridge Crystallographic Data Centre (CCDC) queries were performed using Mogul software. “Entries” refers to number of entries in the CCDC. X-ray crystal structure of **12** was obtained and analysed using PyMol.

With S- and Se-matched molecular pairs of Riluzole and Pretomanid in hand, we studied their fundamental physicochemical properties (Table 1). We noted that replacement of O by S and Se increases lipophilicity by about 0.5 logP-units in both cases. Notably, no further increase in lipophilicity was observed in either case going from S to Se. These differences in lipophilicity follow the same trend seen for the structural differences between the chalcogen homologs (*vide infra*). Increased lipophilicity results in a decrease in solubility. This difference is marginal in case of Pretomanid, which has low solubility itself, but is more pronounced in case of the Riluzole homologs. In that case, decreased solubility of the S- and Se-homologs is likely owed to a combination of increased lipophilicity and increased lattice energy, which manifests in higher melting points compared to their OCF<sub>3</sub> parent (ca. 30 °C higher). Again, no further decrease in solubility was observed going from SCF<sub>3</sub> to SeCF<sub>3</sub>. Passive permeability was not significantly affected by replacement of O with the higher chalcogens, as measured in Martin-Darby Canine Kidney cells.

Next, we studied the impact of the chalcogen replacement on *in vitro* ADME properties and off-target activity. Perhaps counter-intuitively to medicinal chemists, we found stability in human liver microsomes not to be impacted by S- and Se-replacement in either case (Table 2). We conclude that the SCF<sub>3</sub> and SeCF<sub>3</sub> groups introduce „nonmetabolizable lipophilicity“, which may improve *in vivo* half-life, an important pharmacological feature that enables low clinical doses.<sup>[13]</sup> Furthermore, we found no flags for inhibition of CYP3A4 for any of the matched molecular pairs of the two drugs. Time-dependent inhibition of CYP3A4 did slightly increase in case of the Riluzole chalcogen isosteres. However, we found the opposite to be true in case of Pretomanid, indicating no general, intrinsic liabilities of the SCF<sub>3</sub> and SeCF<sub>3</sub> groups for CYP3A4 inhibition. Likewise, human plasma protein binding was affected differently in the two test cases: While PPB increased for the Pretomanid analogs, a slight decrease was noted for the Riluzole homologs. Most importantly, we profiled the matched molecular pairs in a principal *in vitro* safety panel to test if replacement of OCF<sub>3</sub> by SCF<sub>3</sub> and SeCF<sub>3</sub> was associated with a change in off-target potency. We found no significant changes in off-target activity in either case, indicating that, in the present case, the SCF<sub>3</sub> and SeCF<sub>3</sub> groups do not carry any intrinsic safety liabilities (see SI for details).

**Table 1.** Basic physico-chemical properties of the chalcogen matched molecular pairs.

Compound	Measured logP	Aq. Sol. pH 6.8 [mM] <sup>[a]</sup>	Melting point [°C] <sup>[b]</sup>	MDCK-LE P <sub>app</sub> A-B <sup>[c]</sup>
Pretomanid	2.2	0.008	149.9	21.1

S-Pretomanid ( <b>15</b> )	2.7	0.005	155.8	15.5
Se-Pretomanid ( <b>8</b> )	2.7	0.007	149.2	13.7
Riluzole	3.2	0.986	118.3	13.1
S-Riluzole ( <b>12</b> )	3.6	0.124	152.0	16.8
Se-Riluzole ( <b>4</b> )	3.6	0.118	161.6	14.2

[a] aqueous solubility of crystalline material in buffer at pH 6.8; [b] measured by Differential Scanning Calorimetry; [c] passive permeability measured in Martin-Darby Canine Kidney Low Efflux cells and expressed in ratio of concentration of chambers A and B. Higher numbers indicate higher passive permeability.

**Table 2.** Advanced in vitro ADME data for the chalcogen matched molecular pairs.

Compound	Cl <sub>int</sub> in HLM [μl/min/mg] <sup>[a]</sup>	IC <sub>50</sub> for CYP3A4 inhibition [μM]	K <sub>obs</sub> for TDI of CYP3A4 [1/min] <sup>[b]</sup>	human plasma protein binding
Pretomanid	<25	>25	0.025	38%
S-Pretomanid ( <b>15</b> )	<25	>25	0.010	60%
Se-Pretomanid ( <b>8</b> )	<25	>25	0.019	61%
Riluzole	38.9	>25	0.007	85%
S-Riluzole ( <b>12</b> )	40.9	>25	0.011	76%
Se-Riluzole ( <b>4</b> )	32.6	>25	0.012	76%

[a] Cl<sub>int</sub>: intrinsic clearance; HLM: human liver microsomes; [b] rate of time dependent enzyme inhibition (TDI).

In summary, we utilized novel photocatalytic and copper-catalyzed methods to rapidly access the S- and Se-homologs of two OCF<sub>3</sub> containing pharmaceuticals. We showed that these isosteric replacements increase lipophilicity of the compound without impacting microsomal stability, qualifying the SCF<sub>3</sub> and SeCF<sub>3</sub> groups as potential handles to increase *in vivo* half-life. Additionally, we demonstrated that chalcogen isosteres of OCF<sub>3</sub> can be used to tweak physicochemical and ADME properties, and that the SCF<sub>3</sub> and SeCF<sub>3</sub> groups do not carry any intrinsic liabilities. This data should put the SCF<sub>3</sub> and SeCF<sub>3</sub> groups on every medicinal chemist's radar.

## Acknowledgements

C.G. held a doctoral fellowship from la region Rhône Alpes. The authors are grateful to the CNRS, ICBMS (UMR 5246), ICL (Institut de Chimie de Lyon) and Pulsalys for financial support. The French Fluorine Network is also acknowledged for its support. We thank Dr. Guillaume Pilet (Université Lyon 1) for collecting the crystallographic data. We are grateful to Dr. S. Skolnik and the PKS group at Novartis for support with generation of the physicochemical and in vitro ADME data. Dr. M. Shultz, Dr. A. Nadipuram, and the referees are acknowledged for valuable suggestions during data analysis and preparation of the manuscript.

**Keywords:** Chalcogen Trifluoromethyl • Synthetic methodology • Medicinal Chemistry • Isosteres • in vivo half-life

- [1] a) P. Kirsh, *Modern Fluoroorganic Chemistry: Synthesis, Reactivity, Applications*, Wiley, *Wheinem*, **2013**; b) J. Wang, M. Sánchez-Roselló, J. L. Aceña, C. del Pozo, A. E. Sorochinsky, S. Fustero, V. A. Soloshonok, H. Liu, *Chem. Rev.* **2014**, *114*, 2432-2506; c) *Modern Synthesis Processes and Reactivity of Fluorinated Compounds: Progress in Fluorine Science* (Eds.: H. Groult, F. Leroux, A. Tressaud), Elsevier, **2016**; d) Y. Zhou, J. Wang, Z. Gu, S. Wang, W. Zhu, J. L. Aceña, V. A. Soloshonok, K. Izawa, H. Liu, *Chem. Rev.* **2016**, *116*, 422-518.
- [2] N. A. Meanwell, *J. Med. Chem.* **2018**, *61*, 5822-5880.
- [3] a) F. R. Leroux, B. Manteau, J.-P. Vors, S. Pazenok, *Beilstein J. Org. Chem.* **2008**, *4*, 13; b) T. Besset, P. Jubault, X. Pannecoucke, T. Poisson, *Org. Chem. Front.* **2016**, *3*, 1004-1010; c) A. Tili, F. Toulgoat, T. Billard, *Angew. Chem. Int. Ed.* **2016**, *55*, 11726-11735; *Angew. Chem.* **2016**, *128*, 11900-11909.

- [4] a) X.-H. Xu, K. Matsuzaki, N. Shibata, *Chem. Rev.* **2015**, *115*, 731-764; b) S. Barata-Vallejo, S. Bonesi, A. Postigo, *Org. Biomol. Chem.* **2016**, *14*, 7150-7182; c) F. Toulgoat, T. Billard in *Modern Synthesis Processes and Reactivity of Fluorinated Compounds* (Eds.: H. Groult, F. R. Leroux, A. Tressaud), Elsevier, **2017**, pp. 141-179.
- [5] A. Tlili, E. Ismalaj, Q. Glenadel, C. Ghiazza, T. Billard, *Chem. Eur. J.* **2018**, *24*, 3659-3670. Selected references: a) M. Aufiero, T. Sperger, A. S. K. Tsang, F. Schoenebeck, *Angew. Chem. Int. Ed.* **2015**, *54*, 10322-10326; *Angew. Chem.* **2015**, *127*, 10462-10466 b) Q. Lefebvre, R. Pluta, M. Rueping, *Chem. Commun.* **2015**, *51*, 4394-4397. c) C. Matheis, V. Wagner, L. J. Goossen, *Chem. Eur. J.* **2016**, *22*, 79-82. d) A. B. Dürr, H. C. Fisher, I. Kalvet, K.-N. Truong, F. Schoenebeck, *Angew. Chem. Int. Ed.* **2017**, *56*, 13431-13435; *Angew. Chem.* **2017**, *129*, 13616-13620. e) J.-B. Han, T. Dong, D. A. Vacic, C.-P. Zhang, *Org. Lett.* **2017**, *19*, 3919-3922.
- [6] a) Q. Glenadel, C. Ghiazza, A. Tlili, T. Billard, *Adv. Synth. Catal.* **2017**, *359*, 3414-3420; b) C. Ghiazza, V. Debrauwer, C. Monnereau, L. Khrouz, M. Médebielle, T. Billard, A. Tlili, *Angew. Chem. Int. Ed.* **2018**, *57*, 11781-11785; *Angew. Chem.* **2018**, *130*, 11955-11959.
- [7] H. M. Bryson, B. Fulton, P. Benfield, *Drugs* **1996**, *52*, 549-563.
- [8] a) R. Dawson, A. H. Diacon, D. Everitt, C. van Niekerk, P. R. Donald, D. A. Burger, R. Schall, M. Spigelman, A. Conradie, K. Eisenach, A. Venter, P. Ive, L. Page-Shipp, E. Variava, K. Reither, N. E. Ntinginya, A. Pym, F. von Groote-Bidlingmaier, C. M. Mendel, *Lancet* **2015**, *385*, 1738-1747; b) R. Tasneen, F. Betoudji, S. Tyagi, S.-Y. Li, K. Williams, P. J. Converse, V. Dartois, T. Yang, C. M. Mendel, K. E. Mdluli, E. L. Nuermberger, *Antimicrob. Agents Chemother.* **2016**, *60*, 270-277.
- [9] R.-Y. Tang, P. Zhong, Q.-L. Lin, *J. Fluorine Chem.* **2007**, *128*, 636-640.
- [10] P. Jimonet, F. Audiau, M. Barreau, J.-C. Blanchard, A. Boireau, Y. Bour, M.-A. Coléno, A. Doble, G. Doerflinger, C. Do Huu, M.-H. Donat, J. M. Duchesne, P. Ganil, C. Guérémy, E. Honoré, B. Just, R. Kerphirique, S. Gontier, P. Hubert, P. M. Laduron, J. Le Blevec, M. Meunier, J.-M. Miquet, C. Nemecek, M. Pasquet, O. Piot, J. Pratt, J. Rataud, M. Reibaud, J.-M. Stutzmann, S. Mignani, *J. Med. Chem.* **1999**, *42*, 2828-2843.
- [11] C. Ghiazza, C. Monnereau, L. Khrouz, T. Billard, A. Tlili, *Synthesis*, doi: 10.1055/s-0037-1610322.
- [12] N. A. Meanwell, *J. Med. Chem.* **2011**, *54*, 2529-2591.
- [13] a) F. Broccatelli, I. Aliagas, H. Zheng, *ACS Med. Chem. Lett.* **2018**, *9*, 522-527; b) H. Gunaydin, M. D. Altman, J. M. Ellis, P. Fuller, S. A. Johnson, B. Lahue, B. Lapointe, *ACS Med. Chem. Lett.* **2018**, *9*, 528-533; c) D. A. Smith, K. Beaumont, T. S. Maurer, L. Di, *J. Med. Chem.* **2018**, *61*, 4273-4282.